Phonon-assisted conversion between the Jahn-Teller states of the phosphorescent F center in CaO: Optically detected magnetic resonance under uniaxial stress

C. J. Krap, M. Glasbeek, and J. D. W. Van Voorst
Laboratory for Physical Chemistry, University of Amsterdam, Nieuwe Prinsengracht 126, Amsterdam, The Netherlands
(Received 31 May 1977)

From optically detected magnetic resonance spectra and time-resolved measurements of the phosphorescent F center in a nondegenerate state ([101] stress) and in a doubly degenerate Jahn-Teller state ([100] stress), the static coupling of the photoexcited spin vibronic system to external stress as well as the nature of the dynamics (at 1.5 K) involved in the transitions between the spin-vibronic levels have been studied. To describe the static coupling between the $T_{1u}\otimes e_g$ $(S=1)$ spin vibronic system and strain a spin Hamiltonian was derived. Apart from spin-lattice relaxation within a single vibronic Jahn-Teller state, also another relaxation channel was shown to be operative which consists of a phonon-assisted conversion between different vibronic Jahn-Teller states with conservation of spin-state character.

I. INTRODUCTION

It has been shown by means of optical detection of electron spin resonance in the phosphorescent state of F centers in CaO, that the orbital degeneracy of the ^3P excited state is lifted by a Jahn-Teller coupling to a localized e_g vibrational mode. [1] The observed phenomena could be explained as a response from excited F centers which are either in a ξ, η, or ζ Jahn-Teller state.

By studying the temperature behavior of the intensity of the zero-phonon lines of the phosphorescence spectrum under externally applied pressure the authors confirmed their assignment.[2] From the temperature dependence of the intensity of the two zero-phonon lines, observed under [001] stress, it was also concluded that the relaxation from an energetically higher vibronic Jahn-Teller state into a lower-lying one has to proceed on a time scale of microseconds or less.

Recently, it was shown that excited F centers in CaO are also accessible by magnetic resonance in zero field.[3] Optically detected magnetic resonance (ODMR) in zero field gave two distinct microwave transitions at 1.70 and 1.68 GHz, corresponding, respectively, to a decrease and an increase in the phosphorescence intensity. Phosphorescence microwave double resonance (PMDR) revealed that the zero-phonon line was splitted into three lines with peaks at 5743, 5740, and 5742 Å. The latter line arises from pumping at 1.68 GHz, the outer lines from pumping at 1.70 GHz.

A detailed experimental analysis under high optical resolution using the polarization properties of the emitted light, the different polarizations of the microwave field and the effect of small magnetic fields along the principal axes of the crystal, showed that the situation is rather complex.[4] Since the F centers are subjected to an intrinsic strain present in the crystal, one of the features of the ODMR and PMDR derived from magnetic-field effects was the indication of a radiationless transition between any two vibronic Jahn-Teller states of different energy (due to strain) on a time scale of microseconds with conservation of spin-state character.

A powerful means for studying the distinct relaxation paths within a single Jahn-Teller state and the dynamic coupling among different Jahn-Teller states is the application of an external uniaxial pressure of such a magnitude that the effects of intrinsic strain in the crystal can be ignored. In this paper we report on the ODMR spectra and dynamics of excited F centers in a nondegenerate Jahn-Teller state ([101] stress) and in a doubly degenerate Jahn-Teller state ([100] stress). It will be shown that the experimental data provide information about the static coupling of the spin-vibronic system to externally applied stress as well as about the nature of the dynamics involved in spin-lattice relaxation processes.

The form of the spin Hamiltonian to be used in the particular case of a triply degenerate vibronic system with $S=1$ coupled to an e_g-type strain is considered in terms of a general operator equivalent derived from symmetry arguments alone (Sec. II).

In Sec. III we present details of the experimental procedures and the experimental results are given in Sec. IV. Finally, in Sec. V a discussion is given of the dynamics of internal conversion and spin-lattice relax-

ation of the various spin-levels in the Jahn-Teller states.

II. EQUIVALENT OPERATOR IN THE PRESENCE OF STRAIN

The Hamiltonian representing the vibronic coupling of the T_{1u} orbital state with the normal coordinates Q_θ and Q_ϵ of an e_g vibrational mode is given by

$$H_0 = E_0 + (1/2\mu)[p_\theta^2 + p_\epsilon^2 + \mu^2\omega^2(Q_\theta^2 + Q_\epsilon^2)] + V[(-\tfrac{1}{2}Q_\theta + \tfrac{1}{2}\sqrt{3}Q_\epsilon)L_x^2 + (-\tfrac{1}{2}Q_\theta - \tfrac{1}{2}\sqrt{3}Q_\epsilon)L_y^2 + Q_\theta L_z^2] \quad . \tag{2.1}$$

The notation used is that of Ham.[5] The lowest vibronic state is triply degenerate where the basis vectors ξ, η and ζ correspond to the three tetragonal Jahn-Teller distortions. In first order the effect of strain is taken into account by[5]

$$H_S = V_2[(-\tfrac{1}{2}e_\theta + \tfrac{1}{2}\sqrt{3}e_\epsilon)L_x^2 + (-\tfrac{1}{2}e_\theta - \tfrac{1}{2}\sqrt{3}e_\epsilon)L_y^2 + e_\theta L_z^2] + V_3[e_{23}(L_yL_z + L_zL_y) + e_{31}(L_xL_z + L_zL_x) + e_{12}(L_xL_y + L_yL_x)] \quad , \tag{2.2}$$

where

$$e_{ij} = \frac{1}{2}\left(\frac{\partial u_i}{\partial x_j} + \frac{\partial u_j}{\partial x_i}\right) \quad ,$$

and

$$e_\theta = e_{33} - \tfrac{1}{2}(e_{11} + e_{22}) \quad ,$$

$$e_\epsilon = \tfrac{1}{2}\sqrt{3}(e_{11} - e_{22}) \quad .$$

As was shown by Ham, in the strong Jahn-Teller coupling limit, the effect of terms involving the strain tensor elements of t_{2g} symmetry is negligible, and the only effect of strain is an energy shift of the Jahn-Teller states without modifying their wave functions.

In the absence of strain the degeneracy among the spin levels within a single Jahn-Teller distortion is partially lifted due to the first order effect of the dipolar interaction between the electron spins and the effect of LS coupling in second order.

When strain is nonzero this zero-field splitting is modified. Within the limit of $E_{JT}/\hbar\omega \gg 1$ one expects a secular shift of the spin levels due to the combined action of SS and LS interactions. Rather than going into the details of this, we prefer to proceed with a phenomenological approach which automatically accounts for both types of interactions. We restrict ourselves to the limiting case (which is borne out by the experimental data in this and a following paper[4]) that nonsecular t_{2g}-type interactions are completely quenched. Then the basis $|\nu i\rangle$, with $\nu = \xi$, η, or ζ and $i = x$, y, or z (the $S = 1$ spin functions), should diagonalize the operator equivalent. This condition is fulfilled by, e.g.,

$$O_x = L_x^2(d_{xx}S_x^2 + d_{yy}S_y^2 + d_{zz}S_z^2) \quad , \tag{2.3}$$

where

$$d_{pp} = d_p = \sum_q g_{pq}e_q, \quad e_q = e_{qq} \quad ,$$

and g_{pq} is to be related to an element of the magnetoelastic matrix G.[6] Terms involving higher powers of the elements of the strain tensor will be neglected. Application of the symmetry operations of the O_h point group on O_x generates a number of additional terms which are all quadratic in the orbital operators L_p and also quadratic in the spin operators S_p. The linear combination of the terms thus obtained must be invariant to the cubic-symmetry operations. In this way the number of independent g-matrix elements is reduced to five.

Consider now the spin Hamiltonian for the $|\zeta\rangle$ state as

$$H_\zeta = a_{xx}S_x^2 + a_{yy}S_y^2 + a_{zz}S_z^2 \quad , \tag{2.4}$$

then the magnetoelastic matrix G is here defined by

$$a_{ii} = \sum_k G_{ik}e_k \quad .$$

It was calculated that the elements of the G matrix can be expressed as

$$G_{11} = g_{11} + g_{22}, \quad G_{12} = g_{12} + g_{21} \quad ,$$

$$G_{13} = g_{12} + g_{23}, \quad G_{31} = g_{21} + g_{23}$$

and

$$G_{33} = 2g_{22} \quad .$$

Now two supplementary constraints on the G matrix are introduced: (i) the energy shift shared by all levels out of the set $|\nu i\rangle$ is adopted to be zero, irrespective of the applied strain. This results in $G_{31} = -\frac{1}{2}G_{33}$, and (ii) the sum of the changes due to strain in the spin vibronic energies of the levels $|\nu i\rangle$ is taken to be zero (thereby defining the level of zero energy). This results in $G_{13} = -(G_{11} + G_{12})$.

With these arguments the following equivalent operator is obtained:

$$H = H_0 + H_S + H_1 + H_2 \quad , \tag{2.5}$$

$$H_1 = -D(L_x^2S_x^2 + L_y^2S_y^2 + L_z^2S_z^2) \quad , \tag{2.6}$$

and

$$H_2 = e_\theta[\tfrac{1}{3}(G_{11}-G_{12}-G_{33})(2L_z^2S_z^2-L_x^2S_x^2-L_y^2S_y^2)+(-\tfrac{1}{2}G_{11}-G_{12}-\tfrac{1}{4}G_{33})(L_x^2S_y^2+L_y^2S_x^2)$$
$$+\tfrac{1}{3}(-\tfrac{1}{2}G_{11}-G_{12}-\tfrac{1}{4}G_{33})(L_x^2S_x^2+L_y^2S_y^2+L_z^2S_z^2)+(\tfrac{1}{2}G_{11}+G_{12}-\tfrac{1}{4}G_{33})S^2L_z^2+\tfrac{1}{2}G_{33}L^2S_z^2]$$
$$+(e_\epsilon/\sqrt{3})\{(L_x^2S_x^2-L_y^2S_y^2)(G_{11}-G_{12}-G_{33})+(L_x^2-L_y^2)[(\tfrac{1}{2}G_{11}+G_{12}-\tfrac{1}{4}G_{33})S^2+(\tfrac{1}{2}G_{11}+G_{12}+\tfrac{1}{4}G_{33})S_z^2]$$
$$+(S_x^2-S_y^2)[\tfrac{1}{2}G_{33}L^2+(\tfrac{1}{2}G_{11}+G_{12}+\tfrac{1}{4}G_{33}L_z^2]\} \quad . \tag{2.7}$$

It follows immediately what situations arise when the external uniaxial pressure p is directed along the [100], [101], and [111] crystal axes. The possible splittings of the spin-vibronic levels, their radiative properties [based on the contamination through spin-orbit (SO) coupling with the lowest $^1T_{1u}$ state] and the possible microwave transitions are depicted schematically in Fig. 1.

III. EXPERIMENTAL

Yellow-colored single crystals of CaO were purchased from Spicer Ltd. and mounted in a metal helium cryostat. The crystal was irradiated with light from a 100-W Hg lamp via quartz windows in the walls of the cryostat. The emitted light was resolved by a Monospek 1000 Monochromator (usually at a 90° angle from the exciting light), and detected by a Ga-As (C 31034 RCA) photomultiplier. The crystal was surrounded by a slow-wave helix which was connected by a coaxial line to a Hewlett-Packard HP 8690 microwave sweep oscillator. Microwaves in the range of 1–2 GHz were amplified by a Varian 614A 20-W traveling-wave tube amplifier and square wave modulated at 120 Hz with a 50% duty cycle. The microwave induced change in the photomultiplier output was detected with a PAR HR-8 lock-in amplifier. The experiments were performed at 1.5 K. Stresses up to 20 kg/mm^2 could be realized by means of a device capable of transforming the hydrostatic pressure in a gas chamber into uniaxial stress through a connection with a stainless-steel rod. The bottom end of this rod was sealed to a quartz tail which was positioned on top of the CaO crystal.

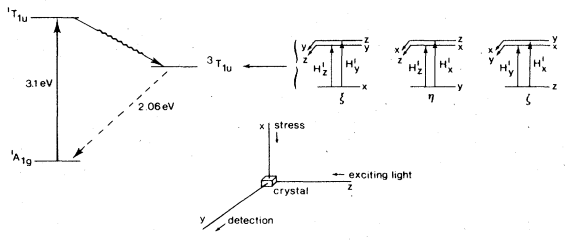

FIG. 1. Term scheme for the electronic states of a F center in CaO, the spin vibronic levels of the $^3T_{1u}$ state are given on an enlarged scale. The laboratory reference frame is as given in the inset. The polarization of the possible microwave transitions is as indicated.

In the time-resolved experiments decay curves were measured using a Varian C-1024 CAT or a PAR boxcar-type 162 system (164 plug-in).

IV. RESULTS

We adopt the laboratory reference frame as depicted in Fig. 1. Then the propagation direction of the exciting light is along the z axis and the phosphorescence is detected along the y direction. The H_1 vector of the microwave field is predominantly along the axis of the helix. The experimental arrangement was such that the system could be excited with x-, y-, or z-polarized microwaves whatever was required for the experiment.

A. [101] stress

With $\vec{p}\,||[101]$, the η state will be lowest,[2] and since the splitting between η and the ξ and ζ states is sufficiently large as compared to kT ($T=1.5$ K), only the zero-phonon emission line of the η state will be observed at higher wavelengths.[2]

The ODMR spectrum was recorded with the microwave field polarized along the [101] direction, i.e., H_1 had components along the x and z directions. The spectrum consists of two unpolarized lines both corresponding to an increase of phosphorescence intensity under microwave resonance.

Since in all other experiments we found no indication for t_{2g}-type strain interactions we attribute the ODMR line splitting to a misalignment which in our experiments was hard to avoid. It is readily verified by looking into the variation of the zero-field splitting parameters as a function of the direction of the applied stress [by means of expression (2.7)] that the sensitivity of the zero-field splittings towards changes in the stress direction is largest for p directed around the [101] directions. Figure 2 gives the value of the resonance frequencies as a function of the applied pressure. A maximum Zeeman splitting was obtained with a magnetic field along the y axis.

By pulsing the resonant microwave power and collecting the light change in the microwave cutoff time, the return of the population of each of the upper spin levels to steady state conditions was studied as a function of time. The effect of a microwave pulse is an increase in the population of the upper spin levels and therefore the change after the pulse is a decay (Fig. 3).

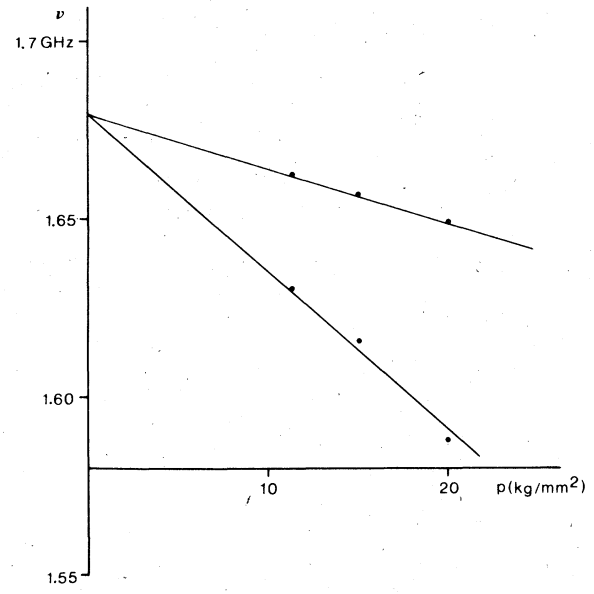

FIG. 2. Microwave resonance frequencies of the $\eta y \rightarrow \eta x$ and $\eta y \rightarrow \eta z$ transitions as a function of applied stress nearly along the [101] direction of the CaO crystal.

Since under continuous illumination the feeding from the ^1P state (or intermediately via a cascade process from the upper ξ and ζ states) will proceed with a constant rate, the decay in the upper spin levels of the lowest Jahn-Teller state can be directly correlated with a spin-lattice relaxation process.

Both upper spin levels of the η state decay exponentially and exhibit the same decay rate. The measured decay times were corrected for the radiative and radiationless decay to the singlet ground state and then plotted as a function of p^2 (Fig. 4). As the energy separation ΔE between the two upper and the lower Jahn-Teller states is linear with p,^{2} it follows that the relaxation rate is proportional to $1/(\Delta E)^2$. Thus coupling between the lowest and highest Jahn-Teller states is a determining factor for the spin-lattice relaxation-rate constant within an isolated Jahn-Teller state.

B. [100] stress

Uniaxial pressure along a cubic axis will cause a splitting of the three degenerate vibronic Jahn-Teller states. For [100] pressure the ξ state shifts to a higher energy and the η and ζ states, which remain degenerate, shift to a lower energy.[2] When the splitting is large as compared to kT only the zero-phonon line of the two lowest Jahn-Teller states will be observable. The microwave field in the helix is not completely linearly polarized and due to this inhomogeneity also microwave transitions with a different polarization can be generated. The response to these small microwave powers will strongly depend upon the actual lifetime of the spin states involved, i.e., transitions to states with a relatively long lifetime will be stronger.

It is to be noted in the following that the y-polarized emission of the ζ x state cannot be detected in the experimental arrangement used.

1. x-polarized microwave field

With an applied pressure of $p = 12$ kg/mm^2, the zero-phonon line is shifted to 5747.4 Å and the ODMR spectrum monitored at this wavelength shows two microwave transitions at 1.59 and 1.69 GHz, respectively (see Fig. 5).

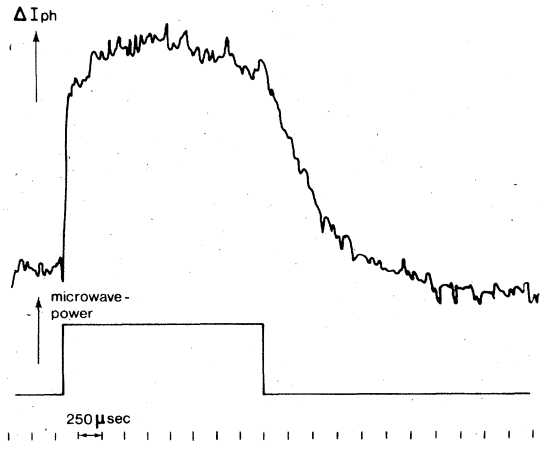

FIG. 3. Time behavior of the light change in a microwave-pulse experiment involving the $\eta y \rightarrow \eta x$ transition in the presence of external stress along the [101] direction.

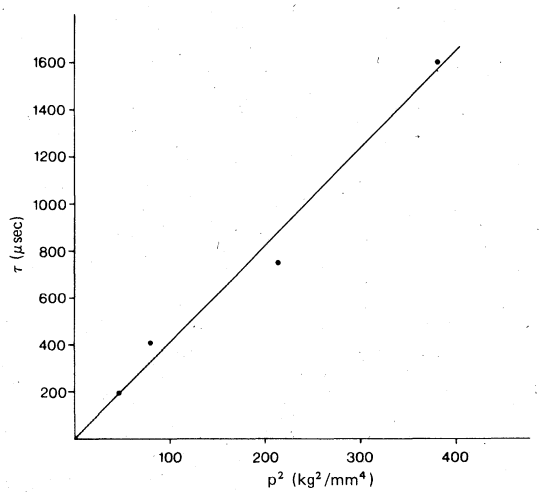

FIG. 4. Pressure dependence of the decay time involving the $\eta y \rightarrow \eta x$ transition in a microwave-pulse experiment ($\vec{p} \| [101]$).

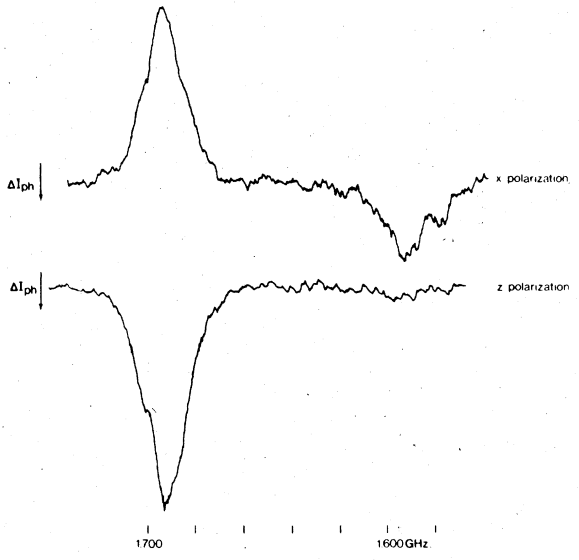

FIG. 5. ODMR spectra recorded under [100] stress ($p = 12$ kg/mm^2) detected at $\lambda = 5747.4$ Å, the polarization of the light changes is as indicated.

The increase in the intensity of the emitted light induced at $\nu = 1.59$ GHz is x polarized and the exponential decay after the microwave pulse is completed, has a characteristic time of 2.2 μsec. According to Fig. 5 the increase in emission at $\nu = 1.69$ GHz is z polarized. Its decay time, however, is three orders of magnitude larger (1200 μsec) and clearly this is why, due to a small inhomogeneity in H_1, this transition is observable (see Fig. 6).

That the z-polarized emission at $\nu = 1.69$ GHz originates from the η state was proven by application of a static magnetic field ($H = 40$ G) along the y axis which removes the resonance from 1.69 GHz (z polarized) to frequencies corresponding to the appropriate Zeeman splitting (mixed polarization). Also in agreement with the level scheme of Fig. 6 it was found that with a magnetic field of 40 G along the y axis as well as along the z axis an x-polarized resonance is found at 1.59 GHz.

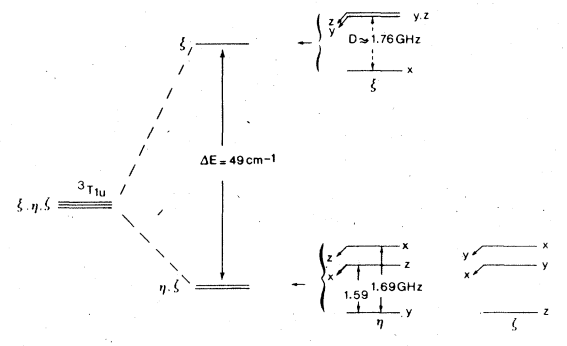

FIG. 6. Energy levels of the F center under [100] stress ($p = 12$ kg/mm^2). The zero-field splittings are shown on an enlarged scale. The D value appropriate to the ξ state has been calculated by means of Eq. (2.7).

On variation of the applied pressure p, the resonance frequency of the $\eta y \rightarrow \eta z$ transition shifts linearly proportional with p whereas the frequency for $\eta y \rightarrow \eta x$ appeared insensitive towards p. It follows from Eq. (2.7) that $G_{33} \approx -2G_{11}$. For uniaxial pressure p along the [100] direction one finds

$$\begin{pmatrix} e_\theta \\ e_\epsilon \end{pmatrix} = (C_{11} - C_{12})^{-1} p \begin{pmatrix} -\frac{1}{2} \\ \frac{1}{2}\sqrt{3} \end{pmatrix} ,$$

where the elements C_{ij} denote the elastic stiffness constants. The shift in the $\eta y \rightarrow \eta z$ transition frequency under [100] stress calculated by means of expression (2.7), then becomes

$$\Delta\nu = (C_{11} - C_{12})^{-1} p (G_{11} - G_{12}) .$$

Since $\Delta\nu = -90$ MHz at $p = 12$ kg/mm^2 and $C_{11} = 20 \times 10^{11}$ dyn/cm^2 and $C_{12} = 6 \times 10^{11}$ dyn/cm^2 for CaO,[7] it is found that $G_{11} - G_{12} = -3.6$ cm^{-1}, where the convention of Fosbergh[8] that a positive stress is a compression has been followed. Alternatively, the stress induced effects may be described in terms of a phenomenological model which describes the effect of strain on the three Jahn-Teller distortions separately.[6] In that case e_{11}, e_{22}, and e_{33}, are taken to be the strain parameters and the magnitude of the components of the magnetoelastic tensor are found to be

$$G_{12}' = G_{33}' = -2G_{11}' = 2.4 \text{ cm}^{-1} .$$

Variation of the applied pressure shows that the decaytime of the x-polarized emission is almost independent of p, while the decaytime of the z-polarized emission with $\nu = 1.69$ GHz is linearly proportional to $(\Delta E)^2$. This indicates that (i) the mechanism for the relaxation of the ηx and ζx states is of the same type as for the ηx state in the case of [101] stress; (ii) the fast relaxation channel of the ηz and ζy states does not involve coupling to an excited vibronic level (no p dependence) and therefore its mechanism is to be developed in terms of the spin states of the *two* degenerate lowest vibronic levels; and (iii) since a fast component in the relatively slow ηx and ζx decay is lacking, the rapid relaxation of the ηz and ζy states is restricted to the participation of only the ηy and ζz states.

Apart from an increase in z-polarized light, the microwave transition at 1.69 GHz also induces a decrease in x-polarized emission (Fig. 5). Since light of this polarization can only originate from the ηz and ζy levels which cannot be pumped at this microwave frequency their change in population must be connected by some relaxation channel to the microwave induced change in the population of the ηy, ηx, ζz, or ζx lev-

els. An interesting observation confirming this, is that the decaytime of the x-polarized emission at 1.69 GHz is of the same order of magnitude as that of the z-polarized emission ($\sim$1200 μsec at 12 kg/mm^2) and follows the same pressure dependence. This is in contrast to the fast pressure independent decay of 2.2 μsec when the ζy and ηz levels are directly pumped by the microwave radiation, and proves that the recurrence towards the equilibrium population is rate determined by the relaxation rate of the ηx and ζx levels into the ζz and ηy levels. The change in population in the ηx and ζx levels on the application of microwave power is essentially an increase, which in turn means a decrease in the population of the nonemitting ηy and ζz levels. Therefore, the depletion of the ηz and ζy levels must be due to the microwave induced depletion of the ηy and ζz levels, from which we know already that their communication with either the ηy and/or ζz is very effective.

2. *y-polarized microwave field*

The zero-field ODMR with a y-polarized microwave field is shown in Fig. 7. In agreement with the short lifetime of the ηz and ζy levels, no microwave transition at 1.59 GHz due to a small inhomogeneity in H_1 was observed. Again the increase in z-polarized light occurs at 1.69 GHz, accompanied by the decrease in x-polarized light both exhibiting a lifetime in the order of milliseconds for $p > 10$ kg/mm^2 and linearly proportional to $(\Delta E)^2$.

Application of a magnetic field H of 48 G along the y axis will strongly mix the ηz (x-polarized light) and ηx (z-polarized light) states and the microwave transitions from ηy to the mixed spin levels have to occur at 1.792 and 1.518 GHz. However, with $\vec{H} \| \vec{y}$ and a y-polarized H_1 field with $\nu = 1.69$ GHz which can only induce the $\zeta z \rightarrow \zeta x$ transition (which emission is y polarized and cannot be seen) not only a decrease in x, but now also a decrease in z-polarized light was observed. Since only the upper η spin levels can emit z-polarized light, the depletion in their population demonstrates unambiguously a strong dynamic coupling between these levels and the ζz level, which is depleted also due to the $\zeta z \rightarrow \zeta x$ transition.

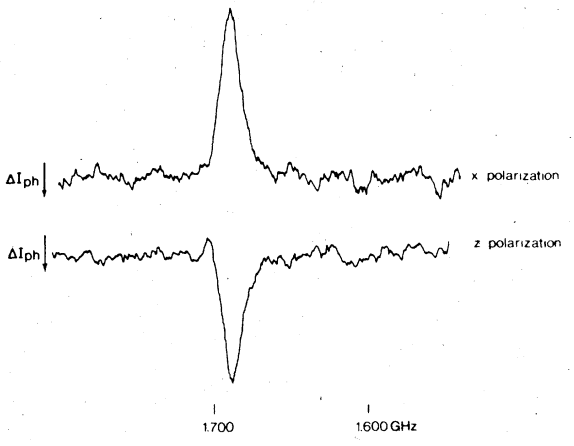

FIG. 7. ODMR spectra in case of [100] stress ($p = 6.7$ kg/mm^2); x and z represent the polarization of the detected light. The microwave field was polarized along the y direction.

In summary the following results were obtained: (a) The $|\eta z\rangle$ and/or $|\zeta y\rangle$ states are dynamically strongly coupled with the $|\eta y\rangle$ and/or $|\zeta z\rangle$ states. This is concluded from microwave pulse experiments performed at zero magnetic field and from the zero-field ODMR lines denoting a decrease in the phosphorescence intensity. (b) The $|\eta x\rangle$ and/or $|\eta z\rangle$ states are strongly coupled to the $|\zeta z\rangle$ state as shown in the experiments with $\vec{H} \| \vec{y}$. From (a) and (b) it is concluded that the fast relaxation has to be attributed to the channels $\eta z \rightarrow \zeta z$ and $\zeta y \rightarrow \eta y$, which is essentially a *phonon-assisted internal conversion between different vibronic Jahn-Teller states with conservation of spin-state character.*

V. DISCUSSION

We first remark that the pressure dependence of the positions and polarizations of the lines in the ODMR spectra as observed for $\vec{p} \| [100]$ and $\vec{p} \| [101]$ is adequately accounted for by use of the operator equivalent of expression (2.7). This means primarily that as long as one is concerned with the properties of the individual vibronic states or their relative energies indeed only e_g-type interactions need consideration and t_{2g}-type interactions are effectively quenched. This situation is representative for the limit of strong Jahn-Teller coupling.[5] However, dynamic processes such as spin-lattice relaxation involve matrix elements nondiagonal in the representation $|\nu i\rangle$ and therefore are a manifestation of the incompleteness of the quenching of t_{2g} interactions.

In general, the mechanism for spin-lattice relaxation (SLR) of paramagnetic centers in ionic solids at $T \lesssim 1.5$ K can be developed in terms of a direct (one-phonon) process.[9] Then the relaxation rate W_{ij} for the transition $|i\rangle \rightarrow |j\rangle$, is given by

$$W_{ij} = (2\pi/\hbar)|M_{ij}|^2 \rho(\hbar\omega_{ij}) \quad , \tag{5.1}$$

where $\rho(\hbar\omega_{ij})$ is the density of phonons of energy $\hbar\omega_{ij}$. In the experiments of Sec. IV, it was found that with $\vec{p} \| [100]$, $\hbar\omega(\eta x \rightarrow \eta y)$ is p independent, and with $\vec{p} \| [101]$, $\hbar\omega(\eta x \rightarrow \eta y)$ changes only slightly with p. Therefore, we take for these transitions $\rho(\hbar\omega_{ij})$ as p independent. Since, on the other hand, $W_{ij} \sim p^{-2}$ it is apparent that M_{ij} is p dependent. This can be seen as follows: Second-order perturbation theory is required in order to simultaneously induce a spin flip and a change in the phonon occupation number by one

quantum unit thus

$$M_{ij} = \sum_k \frac{\langle i|H'|k\rangle \langle k|H'|j\rangle}{\hbar\omega_{ik}} \quad , \tag{5.2}$$

with $H' = H_{0L} + H_{SO} + H_{SS}$.

H_{0L} denotes the Hamiltonian for the coupling between the lattice vibrations and the vibronic levels of the F centers. H_{0L} effectively operates as H_S of Eq. (2.2) the strain now being due to the lattice vibrations.[10] The set $\{|i\rangle\}$ spans the product space of vibronic and phonon wave functions: H_{SO} represents the spin-orbit interaction and H_{SS} is the dipolar interaction between the triplet electron spins. The p dependence of the rate for the $|\eta x\rangle \rightarrow |\eta y\rangle$ relaxation process when $\vec{p}\,\|[101]$ can now be understood on the basis of the effect of H_{SO} as well as H_{SS}: with reference to Fig. 8(a) which is restricted to the effect of p on the vibration*less* vibronic levels. It is easily verified that

$$M^{SO}_{\eta x,\eta y} = \frac{\langle \eta x|H_{0L}|\xi x\rangle \langle \xi x|H_{SO}|\eta y\rangle}{-\Delta} + \frac{\langle \eta x|H_{SO}|\xi y\rangle \langle \xi y|H_{0L}|\eta y\rangle}{-\Delta - \alpha p}$$

$$= \frac{\alpha p}{\Delta^2} \lambda g_L e^{-x} \langle \xi|V_3 e_{12} T_{2\zeta}|\eta\rangle \quad , \tag{5.3}$$

while H_{SS} gives rise to

$$M^{SS}_{\eta x,\eta y} = \frac{2\langle \eta x|H_{SS}|\xi y\rangle \langle \xi|V_3 e_{12} T_{2\zeta}|\eta\rangle e^{-x}}{-\Delta} \quad , \tag{5.4}$$

where in both expressions $x = 3S$, S being the Huang-Rhys factor[5]; it is assumed that $\alpha p << \Delta$. Since Δ is proportional to p and M_{ij} occurs in a quadratic form in Eq. (5.1), both mechanisms predict $W \sim p^{-2}$. However, the H_{SS} contribution to the SLR mechanism is dominant as follows from the experiments with $\vec{p}\,\|[100]$. Then, apart from the above mentioned routes for the $\eta x \rightarrow \eta y$ relaxation [see also Fig. 8(b)] two additional relaxation channels are conceivable, viz., $\eta x \rightarrow \zeta y$ and $\eta x \rightarrow \zeta z$.

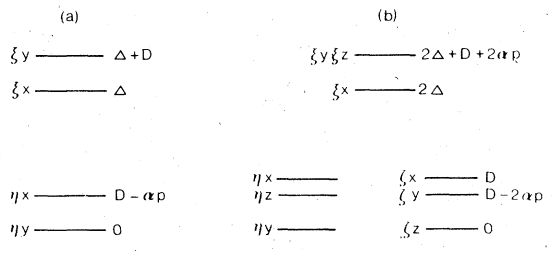

FIG. 8. Schematic energy-level diagram of the F center in the presence of an aribtrary pressure p along (a) the [101] direction, (b) the [100] direction. αp and $2\alpha p$ represent the stress-induced shifts in the zero-field splitting, respectively. Δ accounts for the effect of the V_2 term of expression (2.2).

If H_{SO} were to participate predominantly in SLR, then one finds

$$M^{SO}_{\eta x,\zeta z} = (\lambda g_L e^{-x}/2\Delta) \times \langle \eta|V_3 e_{23} T_{2\zeta}|\xi\rangle \quad . \tag{5.5}$$

By comparison with Eq. (5.3) it is thus found that

$$\frac{M^{SO}_{\eta x,\zeta z}}{M^{SO}_{\eta x,\eta y}} = \frac{\Delta}{2\alpha p} \approx 5 \times 10^3 \quad .$$

A dramatic change in the SLR time is therefore expected for the ηx state in going from a $\vec{p}\,\|[100]$ to a $\vec{p}\,\|[101]$ experiment [the change of $\rho(\hbar\omega_{ij})$ is in comparison negligible]. Since the relaxation rate of the $|\eta x\rangle$ level does not change orders of magnitude by changing the direction of the applied pressure, it is concluded that SLR proceeds predominantly through the participation of the H_{SS} terms.

As noted in Sec. IV the SLR time (τ) of the $|\eta z\rangle$ and $|\zeta y\rangle$ levels in the presence of [100] stress is in the order of microseconds, i.e., three orders of magnitude shorter than the decay times for $|\eta x\rangle$ or $|\zeta x\rangle$.

Now first-order effects contribute to SLR through the V_3 part of H_{0L}:

$$|\eta z\rangle \rightarrow |\zeta z\rangle \quad \text{and} \quad |\zeta y\rangle \rightarrow |\eta y\rangle \quad .$$

Therefore, internal conversion with conservation of spin is a very effective relaxation process.

In the foregoing it was supposed explicitly that the transitions in the relaxation processes are induced by coupling with t_{2g} phonons. Alternatively, it can be imagined that static t_{2g} strain mixes already the $|\nu i\rangle$ states so that now matrix elements involving the coupling with e_g phonons may contribute also in the decay probability.

Essentially, in the latter case the same p dependence for the relaxation rates is expected.

In summary, it was found from the stress dependence of the SLR time that SLR within a single Jahn-Teller state is induced by modulation of the electron spin dipole-dipole interaction through coupling with t_{2g}, respectively e_g, phonons. In case of near degeneracy of Jahn-Teller states internal conversion with conservation of spin-state memory becomes a very effective decay route.

ACKNOWLEDGMENTS

The investigations were supported in part by the Netherlands Foundation for Chemical Research (SON) with financial aid from the Netherlands Organization of Pure Research (ZWO).

[1]P. Edel, C. Hennies, Y. Merle D'Aubigné, R. Romestain, and Y. Twarowski, Phys. Rev. Lett. 28, 1268 (1972).
[2]P. Edel, Y. Merle D'Aubigné, and R. Louat, J. Phys. Chem. Solids 35, 67 (1974).
[3]C. B. Harris, M. Glasbeek, and E. B. Hensley, Phys. Rev. Lett. 33, 537 (1974).
[4]M. Glasbeek, C. J. Krap, and J. D. W. van Voorst (unpublished).
[5]F. S. Ham, Phys. Rev. 138, 1727 (1965).
[6]W. I. Dobrov, Phys. Rev. 134, 734 (1964).
[7]*Landolt-Börstein,* New York, 1969), Group III (Springer-Verlag, Berlin, Heidelberg, New York 1969), Vol. 2, p. 5.
[8]P. W. Fosbergh Jr., Phys. Rev. 93, 686 (1954).
[9]J. H. Van Vleck, Phys. Rev. 57, 426 (1940).
[10]E. B. Tucker, in *Physical Acoustics,* edited by W. P. Mason (Academic, New York, 1966), Vol. IV A, Chap. 2.